

RESEARCH

Open Access



Proteomic profiles screening identified novel exosomal protein biomarkers for diagnosis of lung cancer

Weiyan Feng¹, Ying Lin¹, Ling Zhang² and Weiming Hu^{1*}

Abstract

Background Exosomes play important role in biological functions, including both normal and disease process. Multiple cell types can secrete exosomes, which act as message carriers. Increased evidences reveal that exosomes are promising diagnosis biomarkers in malignant tumors.

Methods In this study, we enrolled 78 participants, including 20 lung adenocarcinoma (LUAD), 18 lung squamous carcinoma (LUSC), 20 lung benign diseases (LUBN) and 20 healthy controls (NL) and we performed parallel reaction-monitoring (PRM)-mass spectrometry to screening the proteomic variation by label free analysis in exosomes from all groups, which has been widely used to quantify and detect target proteins.

Results Total 14 protein were identified as candidate biomarkers, complement components C9, apolipoprotein B (APOB), filamin A (FLNA), guanine nucleotide binding protein G subunit 2 (GNB2), fermitin family homolog 3 (FERMT3) showed significantly differentiation in total lung cancer (LUAD and LUSC together), we then obtained combination analysis of 5 proteins and the area under the curve (AUC), sensitivity (SN) and specificity (SP) were 63.0%, 65.0%, and 75.0%, respectively, in comparison to NL group. And the LUAD combination panel, peroxiredoxin 6 (PRDX6), integrin alpha-IIb (ITGA2B) and hemoglobin subunit delta (HBD) revealed AUC was 95.0%, SN was 90.0% and SP was 95.0% in comparison to NL controls. In LUSC analysis, combination analysis of fibronectin 1 (FN1), pregnancy zone protein (PZP) and complement C1q tumor necrosis factor related protein 3 (C1QTNF3) showed that AUC was 88.1%, SN was 75.0%, SP was 100% in paralleled with NL group. Finally C9, FLNA, PZP were overexpressed in lung cancer H1299 and A549 cell lines and the results indicated that C9 acted as oncogenic role by increasing proliferation, migration and invasion of lung cancer cells, while FLNA and PZP played tumor-suppression by inhibition biological functions of lung cancer cells.

Conclusion Taken together, our study revealed multiple exosomal proteins which could be applied as candidate biomarkers in diagnosis of lung cancer.

Keywords Lung neoplasms, Exosomes, Mass spectrometry, Biomarkers, Multivariate analysis

*Correspondence:

Weiming Hu
huweiming2024@163.com

¹ Department of Pancreas Surgery, West China Hospital, Sichuan University, Chengdu 610051, People's Republic of China

² Division III of General Surgery, West China Hospital-Chengdu Shangjin Nanfu, West China Hospital, Sichuan University, Chengdu 611730, Sichuan, China

Background

Lung cancer is the leading cause of malignant tumor related mortality all over the World and the 5-year survival rate is only 15% [1]. The high mortality of lung cancer is mainly due to late diagnosis because no obvious symptom is observed in early stage of lung cancer. The 5-year survival rate of lung cancer is less than 15% in patients diagnosed at advanced stages, while the survival



© The Author(s) 2025. **Open Access** This article is licensed under a Creative Commons Attribution-NonCommercial-NoDerivatives 4.0 International License, which permits any non-commercial use, sharing, distribution and reproduction in any medium or format, as long as you give appropriate credit to the original author(s) and the source, provide a link to the Creative Commons licence, and indicate if you modified the licensed material. You do not have permission under this licence to share adapted material derived from this article or parts of it. The images or other third party material in this article are included in the article's Creative Commons licence, unless indicated otherwise in a credit line to the material. If material is not included in the article's Creative Commons licence and your intended use is not permitted by statutory regulation or exceeds the permitted use, you will need to obtain permission directly from the copyright holder. To view a copy of this licence, visit <http://creativecommons.org/licenses/by-nc-nd/4.0/>.

rate can reach as high as 80% in those diagnosed at early stage, which highlights the importance of early diagnosis of lung cancer [2]. Although low-dose computed tomography (LDCT) is widely conducted in early screening of lung cancer, high prevalence of false positive is an obstacle in precision diagnosis [3]. In addition, LDCT screening cannot confirm whether early stage lesions detected in asymptomatic patients will finally progress into malignant tumors [4]. The National Lung Screening Trial (NLST) in United States enrolled total 53,454 high risk participants, the results indicated that 22% of non-small cell lung cancer cases detected by LDCT were over-diagnosis. Furthermore, radiation injury and high cost of CT scan have been points of controversy [5].

Exosomes are extracellular vesicles with 40–100 nm diameters and a classic “cup” or “dish” morphology, which are produced by multiple cells including immune cells (reticulocytes, B cells, T cells, mast cells, macrophages etc.) and non-immune cells (epithelial cells, astrocytes, neurons, fibroblasts and tumor cells) [6]. Exosomes have also been found in many bodily fluids such as urine, blood, serum, breast milk, amniotic fluid and cerebrospinal fluid [6]. Exosomes are released by shedding or fusion of multi-vesicular with plasma membrane and play an essential role in intercellular communication by participating in regulation of both normal physiological processes and pathological diseases, including infection and tumor [7]. Production of exosomes contains four steps: initiation, endocytosis, vesicular bodies formation and secretion. And exosomes formation is also regulated by syndecan heparin sulfate proteoglycans and cytoplasmic adaptor syntenin [8]. The fusion of exosomes with cellular membrane of recipient cells leads to release of exosomal contents into cytoplasm by ligand-receptor interactions [9].

One of the most important features is that exosomes presence and stability in most body fluids and resemblance to parental cells in their contents, which enables exosomes act as liquid biopsy specimens for diagnosis of multiples diseases. Exosomes carry multiple molecules, total more than 9000 proteins, 1116 lipid, 3408 mRNA and 2838 microRNAs are contained in exosomes derived from many cell types [10, 11]. The cargoes of exosomes have great potential in acting as biomarkers in diagnosis of diseases due to protection from digestion of various enzymes by lipid bilayer. Among all molecules, exosomal proteins harbor distinct features in comparison to traditional circulating markers because exosomal proteins not only possess higher sensitivity compared with proteins directly from blood but also have higher specificity over secreted proteins. Increased evidences indicate that exosomal proteins can act as biomarkers in diagnosis of multiple tumors [12]. Jakobsen et al. reports that CD317 and

epidermal growth factor receptor (EGFR) from exosomes are valuable biomarkers for diagnosing of non-small cell lung cancer [13]. In pancreatic cancer, circulating exosomal Glypican-1 (GPC1) are extracted from serum of 250 pancreatic patients, which could distinguish between chronic pancreatitis and pancreatic cancer patients in both early and terminal stages [14]. However, the role of exosomal contents in lung cancer diagnosis still remains to be explored.

In this study, we enrolled 78 participants, including 20 lung adenocarcinoma (LUAD), 18 lung squamous carcinoma (LUSC), 20 non-malignant diseases and 20 healthy controls. After isolation and identification of exosomes from plasma of all participants, parallel reaction-monitoring (PRM)-mass spectrometry was conducted to uncover differentially expressed proteins in tumor patients. The aim of this study was to screen and identify exosomal protein biomarkers which could be applied to diagnosis of lung cancer.

Materials and methods

Patients and ethics statement

All treatment-naïve patients were obtained from department of respiratory diseases and thoracic surgery after written informed consent in West China Hospital (Chengdu, China) from 2017–2022. The patients who received any therapy, including surgery, chemical and target therapy were excluded from this study. This study was conducted in agreement with Helsinki Declaration and Approved by Ethical Committee. This study enrolled total of 78 samples, including 20 lung adenocarcinoma (LUAD), 18 lung squamous carcinoma (LUSC), 20 lung benign diseases (LUBN) and 20 healthy controls (NL). All diseases were confirmed by CT and H&E staining. All plasma samples were collected within 2 weeks prior to surgical resection, or radio- and chemotherapy. Healthy controls were from Department of Physical Examination by exclusion of malignancy or benign tumors, as well as family history of tumors and any types of infection. The study design is illustrated in Fig. 1A.

Plasma process, exosome extraction and identification

Plasmas of all groups were collected based on standard protocols, firstly centrifuged at 1600g, 4 °C for 15 min and abandoned red blood cells and leukocytes; and remaining cellular fragments and cell debris were removed in all plasma samples by passing through 0.8 μm filters. The plasma was then transferred to 1.5 mL tubes and refrigerated at -80°C. Exosomes were collected by use of Izon qEV columns by size exclusion chromatography according to the instructions. All isolated exosomes were firstly confirmed by transmission electron microscope (Hitachi, HT7700, Japan) to

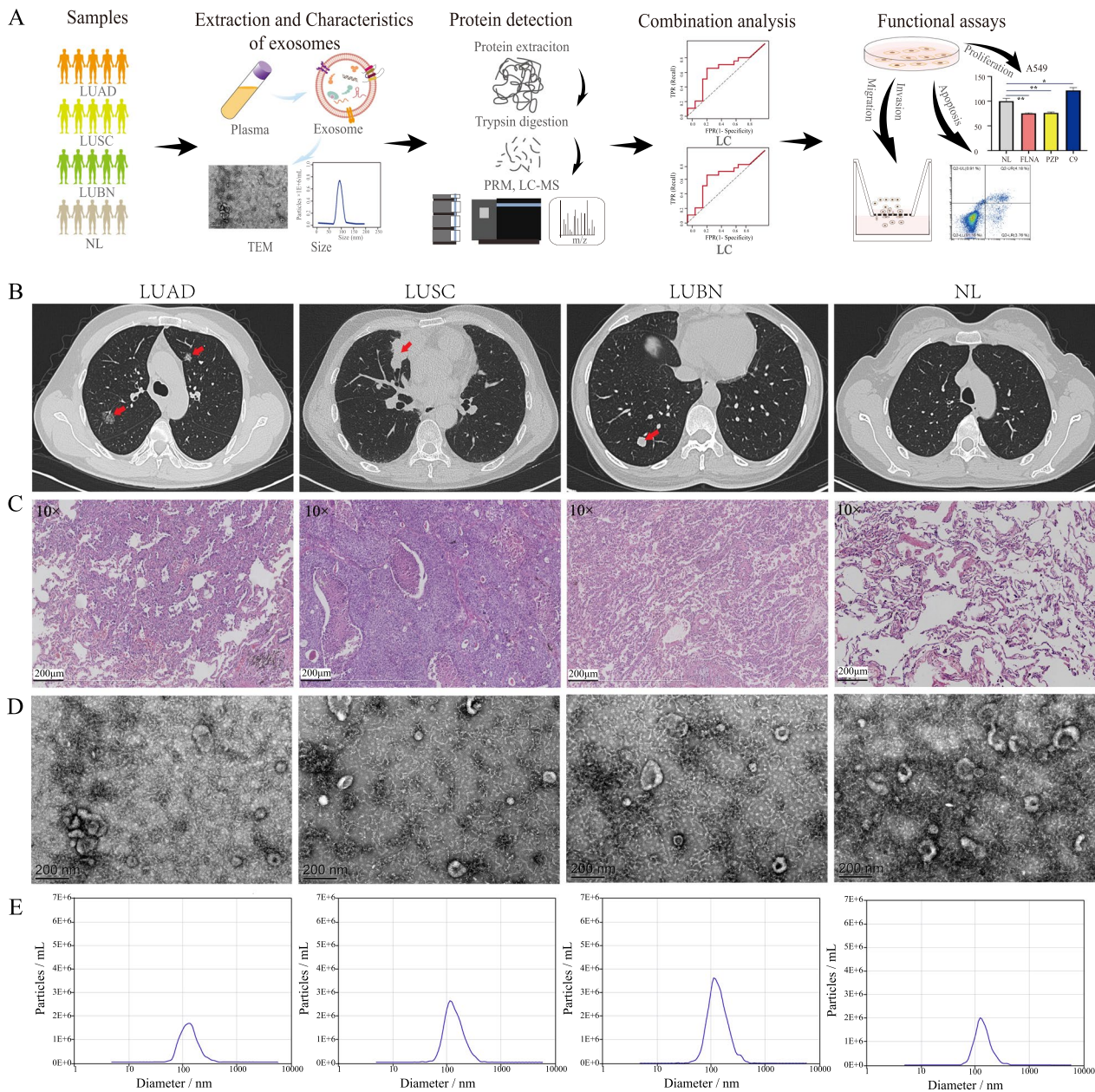


Fig. 1 Study design and exosomes identification. **A** Schematic workflow of study. **B** CT image of representative patients in lung adenocarcinoma (LUAD), lung squamous carcinoma (LUSC), lung benign diseases (LUBN) and healthy controls (NL) groups. **C** Paraffin-embedded tissue was processed for H&E staining. Magnification = ×10, scale bar = 200 μm. **D** Electron microscopy images of plasma exosomes. Bar = 200 nm. **E** Graphics representing size distribution of nanoparticles resulting from with ZetaView PMX 110

observe the double-layer membrane structure and size of 50–100 nm diameters. Besides, we also measured the exosome particle size and concentration using nanoparticle tracking analysis (NTA) with ZetaView PMX 110 (Particle Metrix, Meerbusch, Germany) to confirm the exosomes.

Protein extraction

All samples were grinded by liquid nitrogen into powders and then transferred to centrifuge tubes. Four volumes of lysis buffer (8 M urea, 1% Triton-100, 10 mM dithiothreitol and 1% protease inhibitor cocktail) were then added into powders, followed by three times of

sonication on ice by use of high intensity ultrasonic processor. Centrifugation (Thermo Fisher Scientific, Waltham, MA, USA) (20,000g, 4 °C for 10 min) was performed to remove the remaining debris. All extracted proteins were precipitated in cold trichloroacetic acid (Fortuna Chemical Co. Ltd, Wuhan, China) (TCA, 20%) for 2 h at -20 °C and the supernatant was discarded by centrifuging (12000g) for 10 min at 4 °C. The remaining precipitates were washed three times with cold acetone (Fortuna Chemical Co. Ltd, Wuhan, China). The obtained proteins were re-dissolved in 8 M urea and bicinchoninic acid (BCA) kit (Zhongke Maichen Technology Co., Ltd, Beijing, China) was conducted to test protein concentration according to manufacturer's instruction.

Trypsin digestion

The protein solutions from all groups were reduced with 5 mM dithiothreitol (Beijing BioLab Technology Co., Ltd., Beijing, China) for 30 min at 56 °C, followed by alkylating for 15 min at room temperature in darkness with 11 mM iodoacetamide (Beijing BioLab Technology Co., Ltd., Beijing, China). All protein samples were then diluted to urea concentration less than 2 mM. And first digestion was completed by adding trypsin at 1:50 trypsin-to-protein ratio overnight, the second digestion was performed by 1:100 trypsin-to-protein mass ratios for a second 4 h digestion.

LC-MS/MS analysis

All tryptic peptides were dissolved in 0.1% formic acid (FA) (solvent A) and then loaded directly into a home-made reversed-phase analytical column. The gradient was comprised of an increase 6% to 23% solvent B (0.1% formic acid in 98% acetonitrile) for 38 min, 23% to 35% for 14 min and climbing to 80% for 4 min and finally holding at 80% for last 4 min, all at a constant flow rate of 700 nL/min on EASY-nLC 1000 UPLC system (Thermo Fisher Scientific, Waltham, MA, USA).

The peptides were subjected to NSI source followed by tandem mass spectrometry (MS/MS) in Q Exactive™ Plus (Thermo Fisher Scientific, Waltham, MA, USA) coupled online to the UPLC. The electrospray voltage applied was 2.0 kV. The m/z scan range was 350 to 1000 for full scan, and intact peptides were detected in the Orbitrap at a resolution of 35,000. Peptides were then selected for MS/MS using NCE setting as 27 and the fragments were detected in the Orbitrap at a resolution of 17,500. A data-independent procedure that alternated between one MS scan followed by 20 MS/MS scans. Automatic gain control (AGC) was set at 3E6 for full MS and 1E5 for MS/MS. The maximum IT was set at 20 ms for full MS and auto for MS/MS. The isolation window for MS/MS was set at 2.0 m/z.

The MS data analysis

The MS data of all peptides were processed by Skyline (v.3.6). Peptide settings: enzyme was set as Trypsin (KR/P) and max missed cleavage was set as 2. The peptide length was at 8–25, variable modification was set as carbamidomethyl on Cys and oxidation on Met, and max variable modification was set as 3. Transition settings: precursor charges were set as 2, 3, ion charges were set as 1, 2, ion types were set as b, y, p. The product ions were set as from ion 3 to last ion, the ion match tolerance was set as 0.02 Da. The peptide and protein FDR was set as 1%. All figures were completed by GraphPad 8.0 (GraphPad Software Inc., San Diego, CA, USA).

Differential protein identification

The differential proteins in LC (LUAD and LUSC) groups compared with LUBN and NL groups were calculated as following procedures: where R represents relative proteins quantity and P stands for proteins: $FC_{LC/NL, p} = \text{Mean}(R_{LC, p}) / \text{Mean}(R_{NL, p})$. To amplify differential proteins, FC undergoes log base 2 conversion. After the analysis of differences, the upregulated differential proteins were defined when the P value of t-test < 0.5 and $\text{Log}_2FC > 1.5$, while $\text{Log}_2FC < 1.5$ were down-regulated proteins.

GO/KEGG analysis

Gene Ontology (GO) annotations for all differential proteins are divided into biological processes, cell composition and molecular function. The Kyoto Encyclopedia of Genes and Genomes (KEGG) database is an important network linking know interactions among molecules. The pathway enrichment was considered significant when P value of Fisher's exact test < 0.05.

PPI analysis

Interactions between proteins is analyzed by protein-protein interaction (PPI) software, including direct (physical interactions) and indirect (functional correlations). Differential proteins in LC (LUAD and LUSC) groups compared with NL group were analyzed with the protein network interaction database of STRING (V.11.5).

ROC analysis

Receiver operating Characteristic (ROC) (R Foundation for Statistical Computing, Vienna, Austria) analysis was conducted on the differential proteins by pROC package via R4.0.2 software to assess the sensitivity and specificity. The AUC was used to evaluate the diagnostic value.

Combination analysis model

The model was established by back propagation (BP) neural network (MathWorks, Natick, MA, USA). All

samples were randomly divided into training and testing groups, neural network algorithm was then introduced to establish model by training samples based on selected biomarkers. Finally we performed established model to separate patients and controls in testing group and calculated the area under curve (AUC) value.

In vitro overexpression experiments

Human lung cancer cell lines A549 and H1299 were obtained from the American Type Culture Collection and were authenticated before experiments. Two cell lines were cultured in RPMI-1640 medium (Hyclone, UT, USA, #SH30809.01B) supplemented with 10% fetal bovine serum (ZETA LIFE, CA, USA, #Z7185FBS-500) at 37 °C in humidified incubator with 5% CO₂. Plasmids were synthesized by GeneCopoeia and transfected into A549 and H1299 cells by lipofectamine 3000 (Invitrogen, CA, USA, # L3000015) reagent at a concentration of 1 µg/mL.

Western blot assay

Each group of cells was subjected to lysis on ice with the application of radio immunoprecipitation assay (RIPA) lysate (Thermo Fisher Scientific, Waltham, MA, USA; Cat# 89900) for a period of 10 min. Subsequently, centrifugation was performed at 13,000g for 10 min to facilitate the extraction of total protein. The determination of protein concentration was carried out by employing the bicinchoninic acid (BCA) assay kit. The protein was then combined with the loading buffer and underwent boiling at 100 °C for 5 min to achieve denaturation. Subsequently, 30 µg of protein samples were separated by means of SDS-PAGE and transferred onto a polyvinylidene fluoride (PVDF) membrane (MilliporeSigma, Burlington, MA, USA; Cat# IPVH00010) under an electrical current of 250 mA of assembly (Bio-Rad, USA; Cat# 1703935). The PVDF membrane was blocked using 5% skimmed milk at room temperature for a duration of 1 h. Subsequently, it was incubated with the primary antibodies overnight at 4 °C in a shaker (Scilogex, USA, Cat# SLK-O03000-S). Goat anti-rabbit or mouse IgG (Invitrogen, Carlsbad, CA, USA; Cat# A27039); Goat Anti-Mouse IgG (Invitrogen; Cat# A28177) was utilized as the secondary antibody, and the membrane was incubated with the secondary antibody at room temperature for 2 h. Finally, the membranes were exposed using the enhanced chemiluminescence (ECL) (Bio-Rad Laboratories, Hercules, CA, USA; Cat# 1705060) color solution with the assistance of the Chemiluminescence imager (ChemiScope 6000Touch). The antibodies employed in the experiments were as follows: Anti-FLNA (Proteintech, Wuhan, China, #67133-1-Ig, 1:5000), Anti-PZP (Abcam, Cambridge, UK, #ab233166, 1:1000), Anti-C9 (Abcam, Cambridge, UK,

#ab168345, 1:1000), Anti-GAPDH (Proteintech, Wuhan, China, #60004-1-Ig, 1:10,000), Anti-CD81 (Invitrogen, Carlsbad, CA, USA; Cat# MA5-13548), 1:500), Anti-CD63 (Invitrogen, Carlsbad, CA, USA; Cat# PA5-92370).

Detection of cell viability, migration and invasion

Overexpression and vector-control cells were plated into 96-well plates (1×10^4 cells/well) 24 h post transfection. CCK8 reagent (ZETA) was added into all wells and absorbance values were assayed after 48 h co-cultivation at 450 nm by use of microplate reader (BioTek, Winooski, VT). Migration and invasion were detected by transwell inserts (24-well, 8 µm pore size, Millipore, USA). To perform migration, a medium containing 10% FBS was added to lower chamber and 2×10^4 transfected cells in serum-free medium were cultured in upper chamber. For invasion assays, Matrigel mix (BD Biosciences, CA, USA) was pre-coated in top chamber and 2×10^4 transfected cells were added on the top chamber. Methanol was added to fix the migrated and invaded cells in underside of the membrane and then stained with 0.1% crystal violet for 30 min at RT. Microscope (Leica, Wetzlar, Germany) and Olympus cellSens standard software (v1.5) were performed in image and count of cells, respectively.

Results

Study design, exosomes identification and characterization

In our study, total of 78 participants, including 20 LUAD, 18 LUSC, 20 non-malignant lung diseases (6 hamartoma, 4 atypical hyperplasia, 3 inflammatory pseudotumor, 4 inflammatory nodules and 3 infections) and 20 healthy controls. The clinical features of all participant are illustrated in Table 1. Representative CT images and pathological images of all were groups were shown in Fig. 1B and C, respectively. The exosomes of all groups were firstly identified by transmission electron microscopy (TEM), which was the gold standard to confirm the presence of exosomes. The results revealed that exosomes from all groups were cup-shaped, membrane enclosed vesicles, with 50–150 nm size range and double lipid layer (Fig. 1D), consistent with previous study which described the existence of exosomes. Nanoparticle tracking analysis (NTA) was then applied to analyze the diameter of exosomes and the results indicated the average diameter of exosomes were 100 nm in all groups, which was also consistent with previous study in exosome analysis (Fig. 1E). Finally, specific exosomal biomarkers CD81 and CD63 were detected in 4 randomly selected patients by Western blotting (Supplement Fig. 1). In summary, these results confirmed the purity of exosomes derived from plasmas of all groups in this study.

Table 1 Clinical information of all patients

| Number | Gender | Age | TNM | Stage |
|--------|--------|-----|------------------|-------|
| LUAD | | | | |
| LUAD1 | Male | 48 | T4N1M1A | IVA |
| LUAD2 | Female | 46 | T3N1M0 | IIIA |
| LUAD3 | Female | 49 | T4N1M1A | IVA |
| LUAD4 | Female | 58 | T1cN2M0 | IIIA |
| LUAD5 | Female | 44 | T4NxM1 | IIIA |
| LUAD6 | Male | 50 | T3N1M0 | IIIA |
| LUAD7 | Male | 41 | T1aN0M0 | IA1 |
| LUAD8 | Male | 48 | T4N2M0 | IIIB |
| LUAD9 | Male | 53 | T1cN0M0 | IA3 |
| LUAD10 | Male | 52 | T1cN0M0 | IA3 |
| LUAD11 | Male | 53 | 右上尖后段 T1bN0M0 | IA2 |
| LUAD12 | Male | 48 | T1cNxM1a | IVA |
| LUAD13 | Female | 50 | T2aN0M0 | IB |
| LUAD14 | Female | 54 | T1aN0M0 | IA1 |
| LUAD15 | Male | 46 | T2bN0M0 | IIA |
| LUAD16 | Female | 57 | T1bN0M0 | IA2 |
| LUAD17 | Female | 47 | T1aN0M0 | IA1 |
| LUAD18 | Male | 53 | T2aN2M0 | IIIA |
| LUAD19 | Female | 43 | T4N2M1a | IVA |
| LUAD20 | Male | 45 | T1bN0M0 | IA2 |
| LUSC | | | | |
| LUSC1 | Male | 52 | T2aN0Mx | IIa |
| LUSC2 | Male | 57 | T3N0M0 | IIIB |
| LUSC3 | Male | 63 | T2aN0M0 | IB |
| LUSC4 | Male | 69 | T2aN1M0 | IIIB |
| LUSC5 | Male | 47 | T2aN0M0 | IB |
| LUSC6 | Male | 53 | T2bN0M0 | IIA |
| LUSC7 | Male | 44 | T4N1M1 | IIIA |
| LUSC8 | Male | 61 | T2bN1M0 | IIIB |
| LUSC9 | Male | 77 | T3N1M0 | IIIA |
| LUSC10 | Male | 65 | T1bN0M0 | IA2 |
| LUSC11 | Female | 47 | T3N1M0 | IIIA |
| LUSC12 | Male | 51 | T1cN0M0 | IA3 |
| LUSC13 | Male | 54 | T2aN0M0 | IB |
| LUSC14 | Male | 66 | TisN0M0 | IA1 |
| LUSC15 | Male | 51 | T3N1M0 | IIIA |
| LUSC16 | Male | 59 | T1bN3M0 | IIIB |
| LUSC17 | Male | 61 | T4N0M0 | IIIA |
| LUSC18 | Male | 64 | T2bN2M0 | IIIA |
| LUSC19 | Male | 66 | T2aN0M0 | IB |
| LUSC20 | Male | 59 | T1bN3M0 | IIIB |
| LUBN | | | | |
| LUBN1 | Male | 56 | – | – |
| LUBN2 | Female | 52 | – | – |
| LUBN3 | Male | 44 | – | – |
| LUBN4 | Female | 52 | – | – |
| LUBN5 | Female | 44 | – | – |
| LUBN6 | Female | 41 | – | – |

Table 1 (continued)

| Number | Gender | Age | TNM | Stage |
|--------|--------|-----|-----|-------|
| LUBN7 | Female | 53 | – | – |
| LUBN8 | Male | 55 | – | – |
| LUBN9 | Female | 45 | – | – |
| LUBN10 | Male | 58 | – | – |
| LUBN11 | Female | 36 | – | – |
| LUBN12 | Female | 47 | – | – |
| LUBN13 | Female | 52 | – | – |
| LUBN14 | Female | 38 | – | – |
| LUBN15 | Female | 54 | – | – |
| LUBN16 | Female | 64 | – | – |
| LUBN17 | Female | 63 | – | – |
| LUBN18 | Male | 42 | – | – |
| LUBN19 | Female | 53 | – | – |
| LUBN20 | Male | 47 | – | – |
| Normal | | | | |
| NL1 | Female | 48 | | |
| NL2 | Female | 30 | | |
| NL3 | Female | 45 | | |
| NL4 | Female | 49 | | |
| NL5 | Female | 47 | | |
| NL6 | Female | 31 | | |
| NL7 | Female | 38 | | |
| NL8 | Female | 28 | | |
| NL9 | Female | 35 | | |
| NL10 | Female | 47 | | |
| NL11 | Female | 36 | | |
| NL12 | Female | 35 | | |
| NL13 | Female | 48 | | |
| NL14 | Female | 31 | | |
| NL15 | Female | 31 | | |
| NL16 | Female | 46 | | |
| NL17 | Male | 31 | | |
| NL18 | Male | 42 | | |
| NL19 | Male | 35 | | |
| NL20 | Male | 34 | | |

The characteristics analysis of enrolled molecules in detected panel

The procedure of selecting candidate biomarkers is following: firstly we identified total of 1403 proteins in plasma exosomes and quantification information were obtained in 1059 proteins. Then the cut-off fold was set as 1.5-fold and the significance threshold was $p < 0.05$. Bioinformatic analysis was applied to reveal the functional characteristics of all enrolled molecules. In first analysis, we observed that all 52 proteins were dominated mainly in extracellular (17 proteins) and cytoplasm (12 proteins), while 7 proteins belonged to plasma membrane,

6 proteins related closely to nucleus, 4 proteins and 3 proteins were distributed to mitochondria and endo-reticulum, respectively (Fig. 2A). Kyoto Encyclopedia of Genes and Genomes (KEGG) pathway analysis indicated that these molecules associated closely with tumorigenesis and metastasis in malignant tumors, such as extra-cellular matrix (ECM)-receptor, adipocytokine pathway,

cholesterol, focal adhesion, phagosome, phosphatidylinositol 3 kinase (PI3K)-protein kinase B (AKT) pathway and Rap 1 pathway were all included in top 20 enriched pathways (Fig. 2B). GO annotation indicated that biological process (BP), cellular component (CC) and molecular function (MF) were the most enriched terms (Fig. 2C). In biological process, the top five included cellular process,

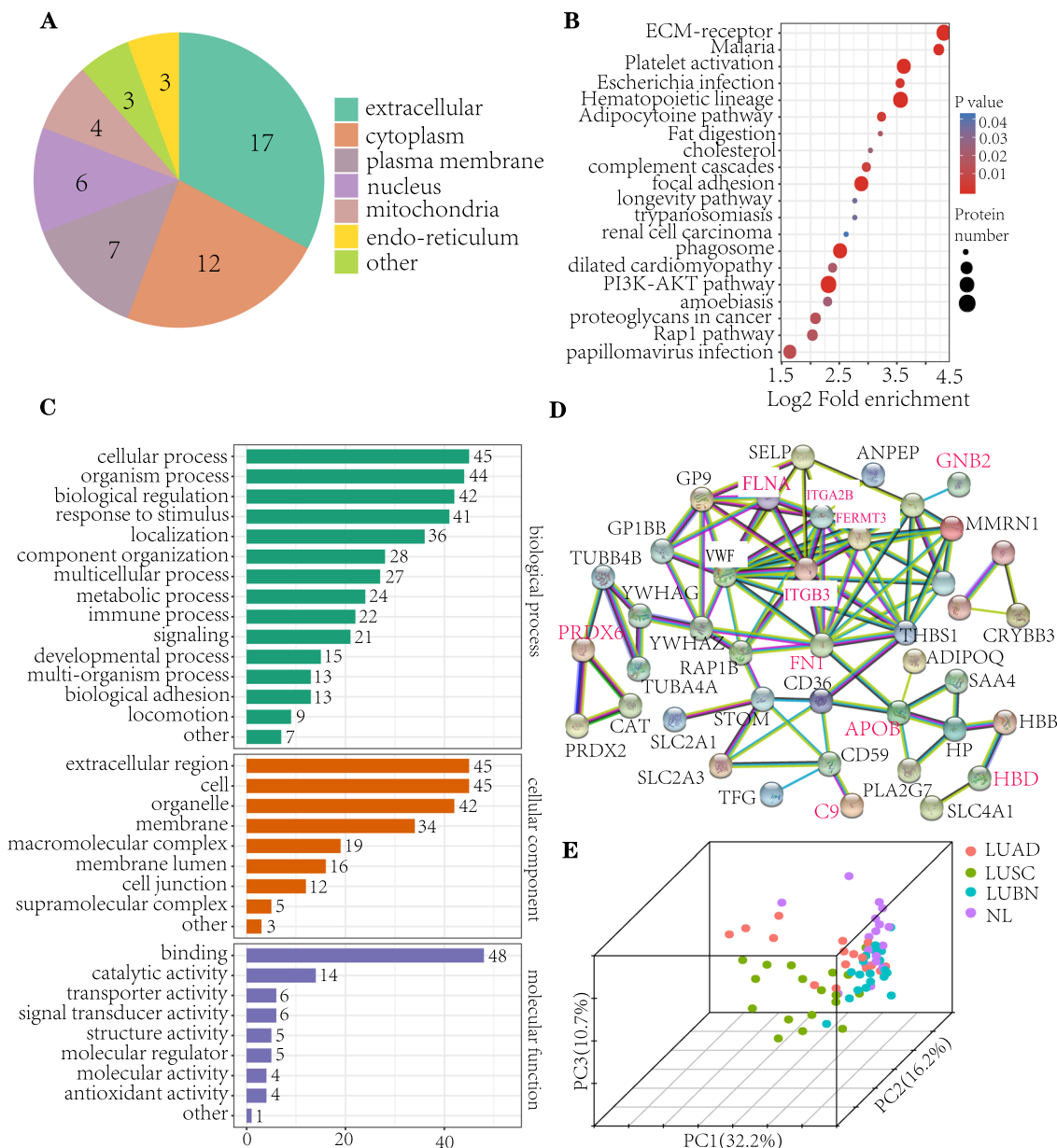


Fig. 2 The characteristics analysis of enrolled molecules in detected panel. **A** Cellular distribution analysis of enrolled proteins in pie diagrams. **B** Analysis of Kyoto Encyclopedia of Genes and Genomes (KEGG) pathway enrichment. **C** Gene ontology (GO) enrichment analysis, including biological processes (top), cellular component (middle) and molecular function (bottom). **D** STRING protein interaction analysis of proteins in detected panel. **E** Principal Component Analysis (PCA) to confirm the general pattern of protein abundance variation among all enrolled groups

organism process, biological regulation, response to stimulus and localization, harbored 45, 44, 42, 41 and 36 proteins, respectively (Fig. 2C). And in cellular component analysis, extracellular region (45 proteins), cell components (45 proteins), organelle (42 proteins) and membrane (34 proteins) were dominated components in compared with macromolecular complex (19 proteins), membrane lumen (16 proteins), cell junction (12 proteins) and supramolecular complex (5 proteins) (Fig. 2C). In molecular function analysis, majority proteins (48 proteins) were acted as binding activity, and 14 proteins harbored catalytic activity. In addition, these proteins also involved in transporter activity (6 proteins), signal transducer activity (6 proteins), structure activity (5 proteins), molecular regulator (5 proteins), molecular activity (4 proteins) and antioxidant activity (4 proteins) (Fig. 2C). To reveal the relationships of all 53 proteins, we constructed the interaction networks based on STRING (v11.0) protein–protein interaction (PPI) dataset. The result yielded a highly clustered network including 5 nodes with 10 edges (clustering coefficient: 0.643, enrichment p -value < 0.05) and we observed that filamin A (FLNA), fermitin family homolog 3 (FERMT3), integrin beta-III (ITGA2B) (ITGB3) and fibronectin 1 (FN1) acted as key molecules in protein interaction (Fig. 2D). Finally, a three-dimensional Principal Component Analysis (PCA) was performed to confirm the general pattern of protein abundance variation among all enrolled groups. Based on quantified proteins of all samples, the results indicated that these proteins showed obvious separation not only between malignant and non-malignant groups (LUAD, LUSC vs LUBN, NL), but between different lung cancer subtypes (LUAD vs LUSC), while no obvious difference was observed between LUBN and NL groups (Fig. 2E).

The role of specific exosomal proteins in diagnosis of lung cancer

Based on parallel reaction-monitoring (PRM)-mass spectrometry assay and functional alterations observed in our screening study, we then explored exosomal proteins which could be acted as candidate biomarkers in diagnosis of lung cancer. Our results revealed 5 target proteins among total lung cancer (LC) (including LUAD and LUSC), LUBN and NL groups according to selection criteria (Fold change > 1.5, p < 0.05). In all candidate proteins, the top 5 were C9, APOB, FLNA, GNB2 and FERMT3 (others were not listed in this study). The C9 and APOB increased dramatically in LC group compared with LUBN (both p < 0.01) and NL groups (both p < 0.01) (Fig. 3A, top). The level of FLNA increased significantly in LC compared to NL group (p < 0.01), but showed decline expression level compared to LUBN (p < 0.05). In

addition, GNB2 and FERMT3 levels elevated obviously in LC patients in comparison to NL group (GNB2: p < 0.05, FERMT3, p < 0.01) (Fig. 3A, top).

To further explore the diagnosis accuracy of candidate biomarkers in lung cancer, we performed receiver operating characteristic (ROC) analysis to define the sensitivity (SN) and specificity (SP) of selected proteins. In C9 analysis, we found that AUC (area under curve) was 71.5%, SN and SP were 42.1% and 95.0% compared with NL group (Fig. 3A bottom). When compared with LUBN, the result revealed that AUC was 73.0%, SN was 42.1% and SP was 95.0% (Fig. 3B). In APOB analysis, the AUC was 73.9%, SN was 42.1%, SP was 95.0% between LC and NL group (Fig. 3A bottom), while in contrast to LUBN, AUC was 71.8%, SN was 26.3% and SP was 95.0% (Fig. 3B). And FLNA exhibited higher SN/SP than C9 and APOB, which revealed AUC 87.0%, SN 63.2%, SP 95.0% between LC and NL (Fig. 3A, bottom). In parallel with LUBN, the AUC was 71.0%, SN was 47.4% and SP was 95.0% (Fig. 3B). In GNB2 analysis, we also found high diagnosis accuracy in LC, the AUC was 82.6%, SN was 68.4% and SP was 95.0% (Fig. 3A, bottom). The highest SN/SP was observed in FERMT3, the AUC was 87.0%, SN 73.7% and SP was 95.0% (Fig. 3A, bottom).

Single biomarker showed limited value in lung cancer diagnosis, combination analysis was very important. In our study, we established combination diagnosis models by back propagation (BP) neural network. Firstly, C9, APOB and FLNA were enrolled to construct combination model for LC vs LUBN, and the results indicated that AUC was 58.5%, SN was 100% and SP was 30% (Fig. 3C, left). And the combination analysis model between LC and NL included C9, APOB, FLNA, GNB2 and FERMT3, this model showed that AUC was 63.0%, SN was 65.0% and SP was 75.0%.

In summary, we screened and identified multiple exosomal proteins in malignant lung tumor compared with LUBN and NL groups, which might be potential candidate biomarkers in future diagnosis of lung cancer.

Validation of novel exosomal biomarkers in diagnosis of LUAD and LUSC

LUAD and LUSC are two major subtypes (LUAD: 50%, LUSC: 20–30%) of lung cancer [15], so it is important to select high specificity and sensitivity biomarkers for LUAD and LUSC, respectively. In LUAD group, we found that PRDX6, ITGA2B and HBD were significantly increased in NL group (all p < 0.01), but showed no obvious differences compared with LUBN (Fig. 4A, top). We also conducted receiver operating characteristic (ROC) analysis in all candidate proteins and the results revealed that in PRDX6 analysis, AUC was 93.6%, SN was 85.0% and SP was 95.0% in comparison

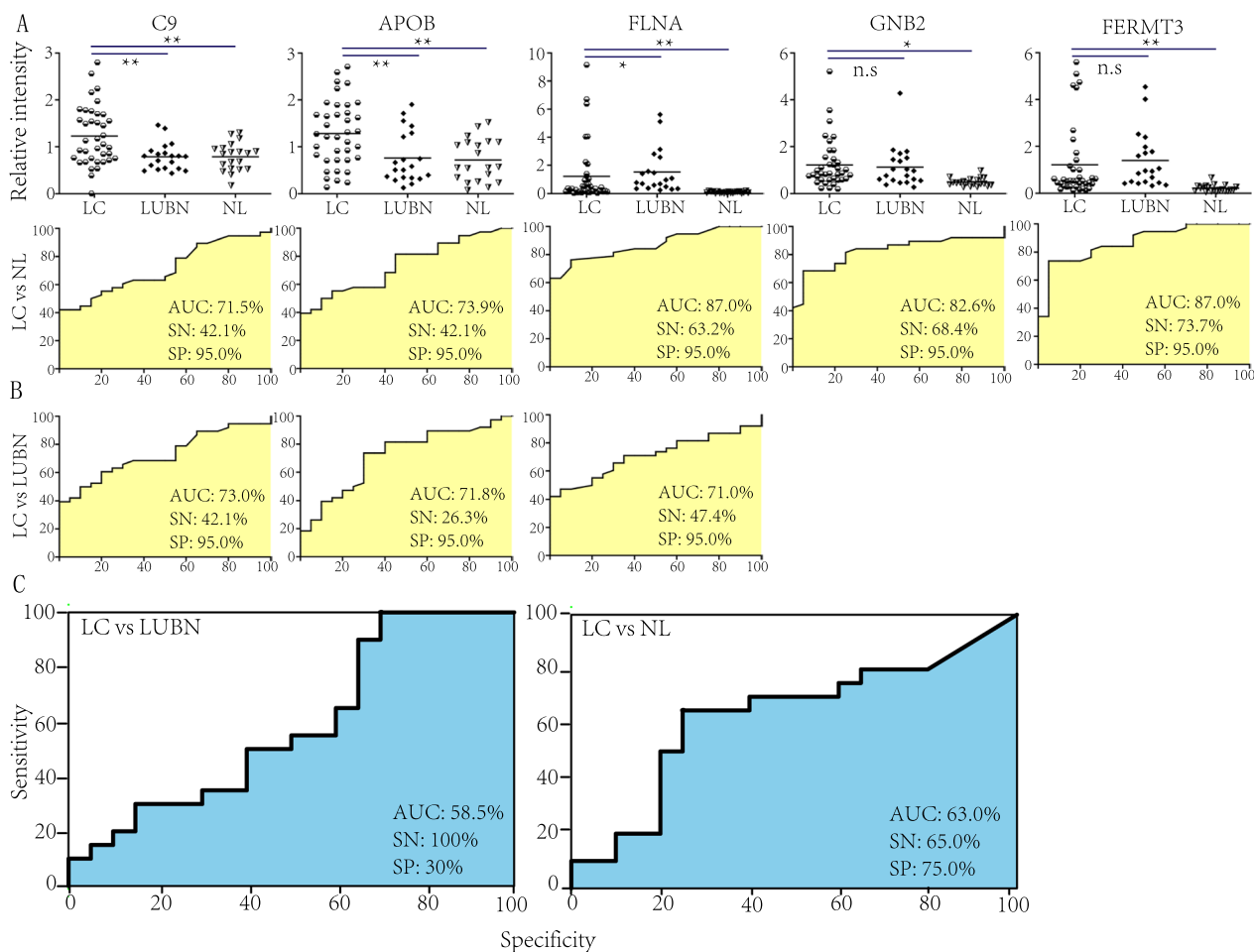


Fig. 3 The concentration and ROC analysis of differential proteins in all lung cancer patients. **A** Concentration (top) of differential biomarkers and ROC analysis (bottom) between lung cancer (LC) and healthy control (NL) controls. **B** ROC curve analysis of LC patients in comparison to LUBN. **C** Combination analysis of C9, APOB, FLNA, GNB2 and FERMT3 in lung cancer (LC) group compared with lung benign diseases (LUBN, left) and healthy control (NL, right) groups. * $p < 0.05$, ** $p < 0.01$, n.s.: none significance

with NL group (Fig. 4A, bottom). In ITGA2B analysis, the AUC was 88.8% and the SN and SP were 80.0% and 95.0%, respectively (Fig. 4A, bottom). And in HBD, we observed that the AUC was 75.1%, SN was 45.0%, SP was 95.0% between LUAD and NL groups (Fig. 4A, bottom).

Next, we investigated the differential proteins which were identified in LUSC patients. We found that FN1, PZP, C1QTNF3, CAVIN2 and HBB showed significantly differentiation in LUSC group. Among 5 proteins, FN1, PZP and C1QTNF3 showed obvious variation in both LUBN and NL, while CAVIN2 and HBB were only observed in NL group. In detail, exosomal levels of FN1, PZP and C1QTNF3 were dramatically declined in LUSC patients when compared with both LUBN (FN1, PZP: both $p < 0.001$, C1QTNF3: $p < 0.05$) and NL (all $p < 0.01$) (Fig. 4B, top), while CAVIN2 and HBB increased significantly only in NL group (Supplement Fig. 2, top).

We also performed ROC analysis and it was showed that in FN1, AUC was 71.4%, SN was 94.4% and SP was 55.0% in LUSC when compared with NL (Fig. 4B, middle), while in comparison to LUBN, the AUC was 99.7%, SN was 100% and SP was 95.0% (Fig. 4B, bottom). In PZP analysis, the AUC was 67.6%, SN was 27.8% and SP was 95.0% compared with NL group (Fig. 4B, middle), and the AUC was 95.4%, SN was 72.2%, SP was 95.0% compared with LUBN (Fig. 4B, bottom). And in C1QTNF3 analysis, AUC was 69.3%, SN was 16.7% and SP was 95.0% between LUSC and NL (Fig. 4B, middle), and AUC was 63.3%, SN was 27.7%, SP was 95.0% in contrast to LUBN (Fig. 4B, bottom). In CAVIN2 and HBB analysis, increased level of CAVIN2 and HBB were observed in LUSC patients compared with NL, while no obvious difference was found between LUSC and LUBN groups (Supplement Fig. 1, top). In ROC analysis, the AUC was 67.1% in CAVIN2; SN was 35.0%

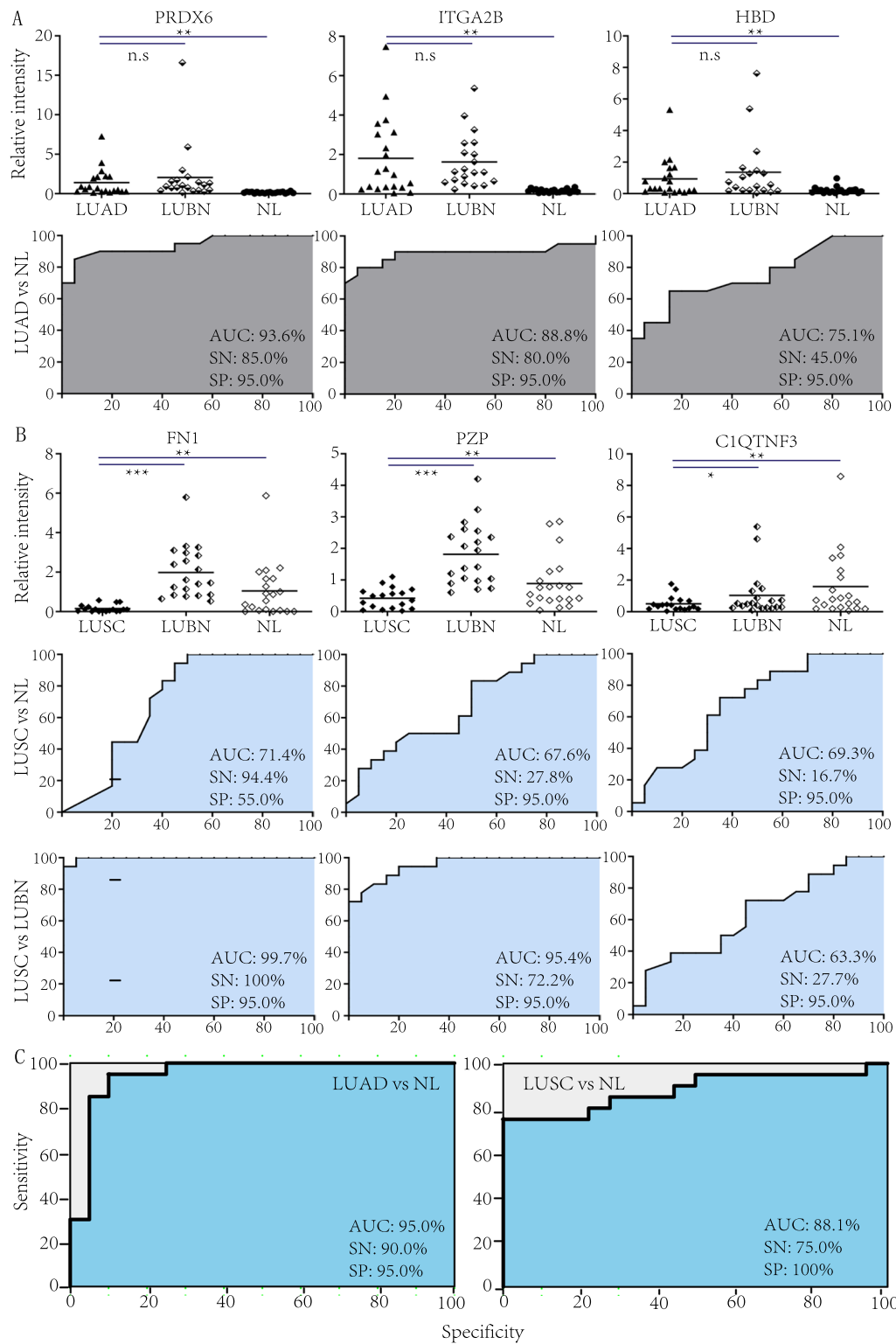


Fig. 4 The concentration and ROC analysis of specific exosomal proteins in lung adenocarcinoma (LUAD) and lung squamous carcinoma (LUSC) patients. **A** Concentration (top) of candidate biomarkers in LUAD, LUBN and NL groups and ROC curve analysis (bottom) between LUAD and NL. **B** Concentration (top) of candidate biomarkers in LUSC, LUBN and NL groups and ROC curve analysis of LUSC vs LUBN (middle), LUSC vs NL (bottom). **C** Combination analysis of PRDX6, ITGA2B and HBD in LUAD patients compared with NL (left) and combination of FN1, PZP, C1QTNF3 in LUSC vs NL group (right). * $p < 0.05$, ** $p < 0.01$, *** $p < 0.001$

and SP was 95.0% (Supplement Fig. 1, bottom). In HBB analysis, AUC was 74.3%, while SN and SP were 45.0% and 95.0%, respectively (Supplement Fig. 2, bottom).

Finally, we also performed combination analysis on LUAD and LUSC. The results indicated that combination of PRDX6, ITGA2B and HBD exhibited high diagnosis value, the AUC was 95.0%, SN was 90.0%, SP was 95.0% in LUAD patients (Fig. 4C, left). And in LUSC analysis, combination of FN1, PZP and C1QTNF3 indicated that AUC was 88.1%, SN was 75.0% and SP was 100% (Fig. 4C, right).

In summary, we identified lung cancer sub-type specific proteins from plasma exosomes, which might be potential candidate biomarkers in LUAD and LUSC diagnosis.

Biological function validation of candidate exosomal proteins

Validation of in vitro biological functions of candidate proteins was performed by overexpression in lung cancer cells. We transfected FLNA, PZP and C9 plasmids into lung cancer H1299 and A549 cells and detected the proteins levels in cell lines 48-h post transfection. Results of western-blot indicated that FLNA, PZP and C9 were highly expressed in both H1299 and A549 cells (Fig. 5A). We then detected cell proliferation ability by CCK8, and the results indicated that overexpression of C9 significantly increased cell viability in H1299 and A549 cells (both $p < 0.05$), while FLNA and PZP dramatically inhibited cell viability in both H1299 and A549 cells (all $p < 0.01$) (Fig. 5B), which suggested the oncogenic role of C9 and anti-tumor effect of FLNA and PZP.

Next, we performed transwell assay to detect the migration and invasion of H1299 and A549 cells in the presence of overexpressed three proteins. In consistent with cell proliferation assay, C9 significantly enhanced migration and invasion of H1299 and A549 cells, while FLNA and PZP suppressed migration and invasion of both cell lines (Fig. 5C and D). The results also suggested the tumor-promotion of C9 and anti-tumor role of FLNA and PZP.

Finally, flow cytometry was conducted to measure the apoptosis. We observed that apoptosis rate dramatically enhanced in FLNA (A549: 13.4%, H1299: 14.2%) and PZP (A549: 17.7%, H1299: 15.3%) in contrast to control group (A549: 9.9%, H1299: 9.8%), and C9 overexpression obviously decreased apoptosis in both A549 (7.4%) and H1299 (8.8%) cells.

Taken together, by in vitro biological function experiments, we confirmed that C9 played tumor-promotion role while FLNA and PZP exhibited anti-tumor effect.

Discussion

Due to lack of effective early diagnostic methods, majority of lung cancer patients are still diagnosed at advanced stage. Thus, it is urgent to seek more valuable biomarkers for early diagnosis of lung cancer. Exosomes are extracellular vesicles and play important roles in biological function regulation and tumor promotion. Exosomes contain multiple cargos, including proteins, microRNAs, DNA and lipids, which are stable in vivo due to protection from double-lipid membranes of exosomes and can be applied as biomarkers for diagnosis of multiple diseases and malignant tumors [12]. The glypican-1 could be applied early diagnose marker for pancreatic cancer [12]. Claudin 4 (CLDN4), epithelial cell adhesion molecule (EPCAM), cluster differentiation 151 (CD151), lectin galactoside binding soluble 3 binding protein (LGALS3BP) and histon H2B (HIST2H2BF) were useful in early detection of PDAC [16, 17]. Besides, the role of exosomes molecules in clinical diagnosis were also identified in breast tumor, [18], polycystic kidney disease (ADPKD) [19], gastric cancer [20] and NSCLC [21].

In this study, we divided 78 clinical plasma samples into LUAD, LUSC, LUBN and NL groups. Parallel reaction monitoring acquisition method (LC-PRM) was conducted to investigate exosomal protein profiles and identify differentiation proteins between tumor (LUAD and LUBN) and control (LUBN and NL). And we revealed 5 proteins (C9, APOB, FLNA, GNB2 and FERMT3) in all lung cancer (LUAD and LUSC), combination analysis indicated that AUC was 63.0%, SN was 65.0%, SP was 75.0% in comparison to NL group. As LUAD (50%) and LUSC (35%) were two major subtypes of lung cancer, we also explored the biomarkers which could be applied specific for LUAD and LUSC. In LUAD, we found that PRDX6, ITGA2B and HBD were specific differentiated in this lung cancer subtype, combination analysis revealed 95.0% AUC, 90.0% SN and 95.0% SP in comparison to NL. And in LUSC, combination analysis of FN1, PZP and C1QTNF3 indicated that AUC was 88.1%, SN was 75.0% and SP was 100% compared with NL. These results suggested that these exosomal proteins could act as candidate biomarkers in future diagnosis of lung cancer.

In all identified proteins, PZP (pregnancy-zone protein) was associated with pregnancy and produced in multiple tissues. And in a study enrolled 35 patients, circulating serum PZP was validated as novel biomarker in lung adenocarcinoma in type 2 diabetes mellitus patients [22]. ITGA2B and FLNA played important roles in metastasis of breast cancer, while increased FLNA and ITGA2B were detected in serum samples from 20 invasive ductal carcinoma breast cancer and 20 female controls by LC-MS analysis [23]. GNB2 was classified

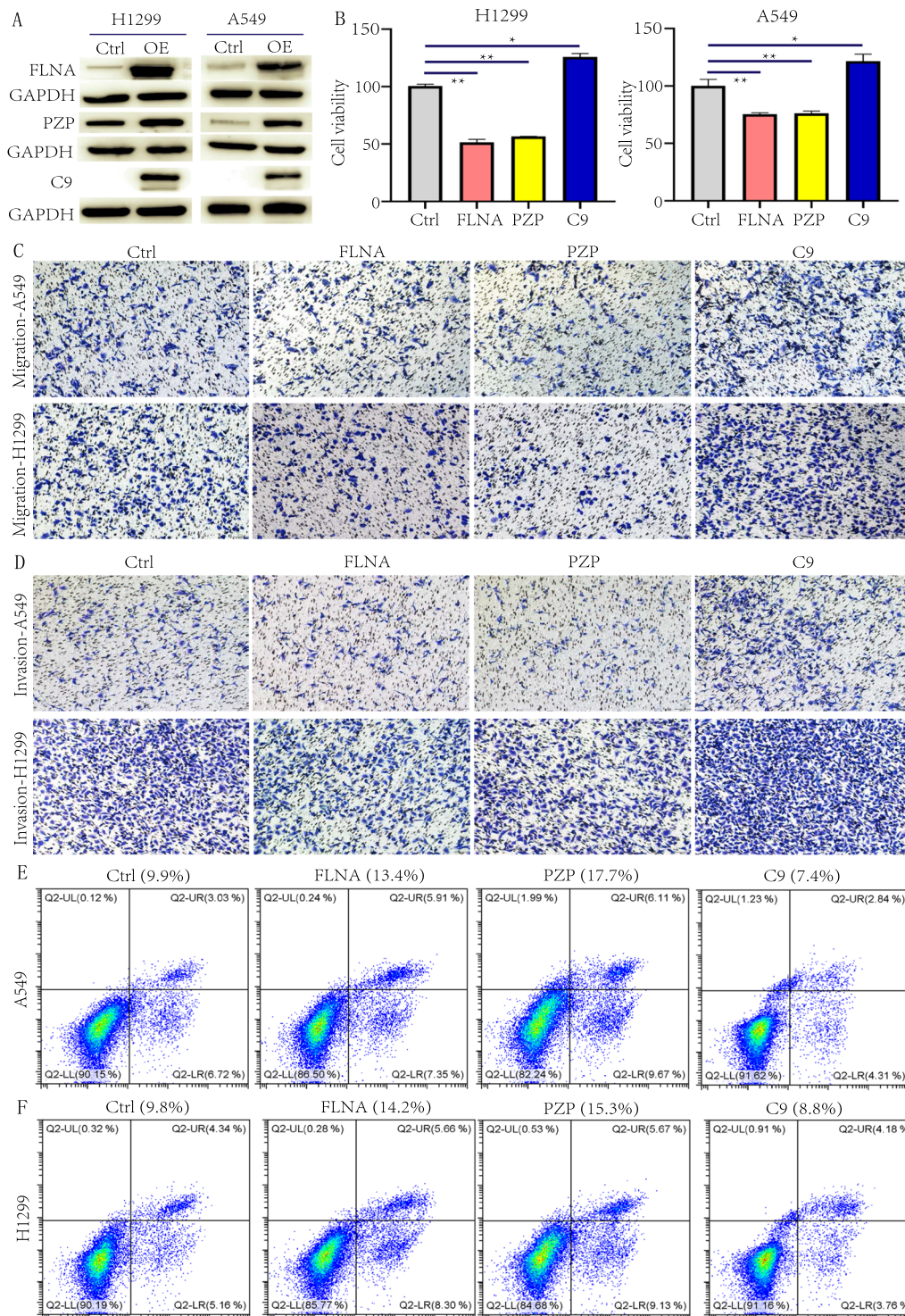


Fig. 5 In vitro biological function validation of candidate biomarkers in lung cancer cell lines. **A** Western blot to detect the overexpression of FLNA, PZP and C9 in H1299 (left) and A549 (right) cells. OE: overexpression, Ctrl: control vector. **B** CCK8 detection for cell viability. * $p < 0.05$, ** $p < 0.01$. **C** Migration (without matrigel) detection of overexpression and control groups. **D** Invasion (with matrigel) detection of overexpression and control groups. **E** Apoptosis assay by flow cytometry between overexpression and control groups

as G-proteins and played an important role in insulin signaling pathway, Saddala et al. revealed that decreased GNB2 was detected in placental growth factor ablated Akita diabetic mice and involved in insulin resistance [24]. FN1 was a glycoprotein which involved in cell adhesion and migration processes including wound healing, blood coagulation and metastasis. FN1 was suggested as candidate biomarker in various cancers and promoted metastasis of lung cancer cells by activating focal adhesion kinase (FAK) signaling pathway [25]. FERMT3 had a key role in regulation of hemostasis and acted as nodule of interaction network in bifendate-mediated therapy of acute liver injury [26]. CAVIN2 was a member of cardiac syndecan-2 interactome and involved in cytoskeletal remodeling and protein metabolism [27]. C9 was a member of complement family and was one of the component proteins of membrane attack complex (MAC) in complement cascades. Label-free proteomics analysis indicated that C9 level dramatically increased in plasma of gastric cancer patients, as well as in tumor tissues and cell lines [28]. In rat model, the results also indicated up-regulation of C9 gene expression in esophageal adenocarcinoma compared with non-cancer epithelial cells [29]. Besides, Chantaraamporn et al. confirmed elevated C9 expression in colorectal cancer patients, which confirmed the important role of C9 in tumor diagnosis [30]. C1QTNF3 associated closely to bleeding disorder and chromosome 5P13 duplication syndrome, while increased C1QTNF3 was found in bowel metastasis ovarian cancer [31]. APOB located on chromosome 2p24.1 and was the main apolipoprotein of chylomicrons and low-density lipoprotein, Dent et al. showed that single nucleotide polymorphism (rs1801701C>T) was significantly associated with NSCLC survival, which indicated that role of APOB genetic variants in tumor progression [32].

Previous report revealed that protein biomarkers from plasma exosomes played critical roles in lung cancer diagnosis [33], and our study revealed several novel exosomal protein biomarkers not only for early diagnosis of lung cancer but also for specific lung cancer subtype (LUAD and LUSC). Previous studies revealed several tumor associated proteins, including EGR, KRAS, extracellular matrix metalloproteinase inducer (EMMPRIN), claudins and RAB-family proteins [34], as well as microRNA (let-7f, miR-20b and miR-30e-3p) [35] from exosomes could be applied in NSCLC diagnosis. However, our study uncovered novel protein biomarkers which were specific for different lung cancer subtypes LUAD (PRDX6, ITGA2B, HBD) and LUSC (FN1, PZP, C1QTNF3), which showed high AUC, SN and SP in comparison to healthy controls and could be helpful in future precision diagnosis of lung cancer. The clinical value of our study is that we provide the candidate and potential biomarkers for

early diagnosis of lung cancer, and we also confirm the role of exosomal molecules in malignant tumor diagnosis. To apply these biomarkers in future clinical usage, we still provide more evidences including large cohort, multi-center clinical trial and the stability of this panel. The limitation of this study was small cohort of plasma samples (78 cases) and future validation should involve large number of participates for all groups, as well as multi-center clinical trials.

Conclusions

In summary, our study provided an extensive approach to screening exosomal-derived biomarkers for lung cancer. Our study indicated that based on proteomic profiling, plasma-derived exosomal proteins could act as ideal non-invasive biomarkers for diagnosis of lung cancer. Importantly, combination of these novel protein biomarkers showed great potential in detection of lung cancer, especially in distinguishing lung cancer and non-malignant lung diseases. And the functional and molecular mechanisms of these exosomal proteins should be further investigated.

Abbreviations

| | |
|---------|--|
| NSCLC | Non-small cell lung cancer |
| LC | Lung cancer |
| LUAD | Lung adenocarcinoma |
| LUSC | Lung squamous carcinoma |
| LUBN | Lung benign diseases |
| NL | Normal healthy control |
| PRM | Parallel reaction monitoring |
| AUC | Area under the curve |
| SN | Sensitivity |
| SP | Specificity |
| LDCT | Low dose computed tomography |
| APOB | Apolipoprotein B |
| FLNA | Filamin A |
| GNB2 | Guanine nucleotide-binding protein G |
| FERMT3 | Fermitin family homolog 3 |
| PRDX6 | Peroxisredoxin 6 |
| ITGA2B | Integrin alpha-IIb |
| HBD | Hemoglobin subunit delta |
| FN1 | Fibronectin 1 |
| PZP | Pregnancy zone protein |
| C1QTNF3 | Complement C1q tumor necrosis factor-related protein 3 |
| CAVIN2 | Caveolae-associated protein 2 |
| HBB | Hemoglobin subunit beta |

Supplementary Information

The online version contains supplementary material available at <https://doi.org/10.1186/s12014-025-09535-7>.

Supplementary Material 1. Figure 1. Detection of exosomal positive protein markers CD81 and CD63 by Western blotting, and the GAPDH was performed as internal control.

Supplementary Material 2. Figure 2. The concentration (Top) and ROC (Bottom) analysis of CAVIN2 and HBB in LUSC patients. **p<0.01.

Acknowledgements

We thanks medical record department for providing information of patients

Author contributions

WH designed the manuscript, WF performed data analysis and wrote the manuscript, YL collected samples and help to complete manuscript, LZ conceived of the study and participated in designation.

Funding

None.

Availability of data and materials

No datasets were generated or analysed during the current study.

Declarations**Ethics approval and consent to participate**

This study was approved by ethics committee of West China Hospital.

Consent for publication

Not applicable.

Competing interests

The authors declare no competing interests.

Received: 1 November 2024 Accepted: 25 March 2025

Published online: 15 April 2025

References

- Qi J, Li M, Wang L, Hu Y, Liu W, Long Z, et al. National and subnational trends in cancer burden in China, 2005–20: an analysis of national mortality surveillance data. *Lancet Public Health*. 2023;8:e943–955.
- Meyer ML, et al. New promises and challenges in the treatment of advanced non-small-cell lung cancer. *Lancet*. 2024;404:803–22.
- Wang L, Qi Y, Liu A, et al. Opportunistic screening with low-dose computed tomography and lung cancer mortality in China. *JAM Netw Open*. 2023;6:e2347176.
- Adams S, et al. Lung cancer screening. *Lancet*. 2023;401:1390–408.
- Alberle DR, Adams AM, Berg CD, Balck WC, Clapp JD, Fagerstrom RM, et al. Reduced lung-cancer mortality with low-dose computed tomographic screening. *N Eng J Med*. 2011;365:395–409.
- Zhong DY, Wang ZY, Ye ZC, Wang YF, Cai XJ. Cancer-derived exosomes as novel biomarkers in metastatic gastrointestinal cancer. *Mol Cancer*. 2024;23:67.
- Asleh, Dery V, Taylor C, Davey M, Djeungoue-Petga M, Ouellette RJ. Extracellular vesicle-based liquid biopsy biomarkers and their application in precision immune-oncology. *Biomarker Res*. 2023;11:99.
- Wang H, Zhang Y, Zhang H, Cao H, Mao JN, Chen XX, et al. Liquid biopsy for human cancer: cancer screening, monitoring and treatment. *MedComm*. 2024;5:e564.
- Liang HY, Zhang LY, Rong J. Potential roles of exosomes in the initiation and metastatic progression of lung cancer. *Biomed Pharmacother*. 2023;165:115222.
- Ma LW, Guo HL, Zhao YX, Liu ZB, Wang CR, Bu JH, et al. Liquid biopsy in cancer: current status, challenges and future prospects. *Sig Trans Targ Ther*. 2024;9:336.
- Clancy JW, Dsouza-Schorey. Tumor derived extracellular vesicles: multifunctional entities in the tumor microenvironment. *Ann Rev Pthol Mech Dis*. 2023;18:205–29.
- Ma S, Zhou ML, Xu YH, Gu XL, Zou MY, Abudushalamu G, et al. Clinical application and detection techniques of liquid biopsy in gastric cancer. *Mol Cancer*. 2023;22:7.
- Huang SH, Li Y, Zhang JH, Rong J. Epidermal growth factor receptor-containing exosomes induce tumor-specific regulatory T cells. *Cancer Invest*. 2013;31:330–5.
- Melo SA, Luecke LB, Kahlert C, Fernandez AF, Gammon ST, Kaye J, et al. Glypican-1 identifies cancer exosomes and detects early pancreatic cancer. *Nature*. 2015;523:177–82.
- Hendriks LL, Remon J, Faivre-Finn C, Garassino MC, Heymach JV, et al. Non-small-cell lung cancer. *Nat Rev Dis Primers*. 2024;10:71.
- Gastillo J, Bernard V, SanLucas FA, Allenson K, Capello M, Kim DU, et al. Surfaceome profiling enables isolation of cancer-specific exosomal cargo in liquid biopsies from pancreatic cancer patients. *Ann Oncol*. 2018;29:223–9.
- Yang J, Zhang YX, Gao X, Yuan Y, Zhao J, Zhou SQ, et al. Plasma-derived exosomal ALIX as a novel biomarker for diagnosis and classification of pancreatic cancer. *Front Oncol*. 2021;11:628346.
- Chen IH, Xue L, Hsu CC, Sebastian J, Li P, Andaluz H, et al. Phosphoproteins in extracellular vesicles as candidate markers for breast cancer. *Proc Natl Acad Sci*. 2017;114:3175–80.
- Salih M, Demmers JA, Bezstarosti KB, Leonhard WN, Losekoot M, vanKooten C, et al. Proteomics of urinary vesicles links plakins and complement to polycystic kidney disease. *J Am Soc Nephrol*. 2016;27:3079–92.
- Li QE, Shao YF, Zhang XJ, Zheng T, Miao M, Qin LJ, et al. Plasma long noncoding RNA protected by exosomes as a potential stable biomarker for gastric cancer. *Tumor Biol*. 2015;36:2007–12.
- Grimolizzi F, Monaco F, Leoni F, Bracci M, Staffolan S, Bersaglieri C, et al. Exosomal miR-126 as a circulating biomarker in non-small cell lung cancer regulating cancer progression. *Sci Rep*. 2017;5:15277.
- Yang JY, Yang C, Shen H, Wu WJ, Tian Z, Xu QH, et al. Discovery and validation of PZP as a novel serum biomarker for screening lung adenocarcinoma in type 2 diabetes mellitus patients. *Cancer Cell Int*. 2021;21:162.
- Fredolini C, Pathak KV, Paris L, Chapple KM, Tsantilas KA, Rosenow M, et al. Shotgun proteomics coupled to nanoparticle-based biomarker enrichment reveals a novel panel of extracellular matrix proteins as candidate serum protein biomarkers for early-stage breast cancer detection. *Breast Cancer Res*. 2020;22:135.
- Saddala MS, Lennikov A, Grab DJ, Liu GS, Tang SB, Huang H. Proteomics reveals ablation of PIGF increases antioxidant and neuroprotective proteins in the diabetic mouse retina. *Sci Rep*. 2018;8:16728.
- Meng XN, Jin Y, Yu Y, Bai J, Liu GY, Zhu J, et al. Characterisation of fibronectin-mediated FAK signaling pathways in lung cancer cell migration and invasion. *Brit J Cancer*. 2009;101:327–34.
- Talifu A, Saimaiti R, Maitinuer Y, Liu G, Miernisha A, Xin X. Multiomics analysis profile acute liver injury module clusters to compare the therapeutic efficacy of bifendate and muaddil sapra. *Sci Rep*. 2019;9:4335.
- Mathiesen SB, Lunde M, Stensland M, Martinsen M, Nyman TA, Christensen G, et al. The cardiac syndecan-2 interactome. *Front Cell Dev Biol*. 2020;8:792.
- Afshar-Kharghan V. The role of the complement system in cancer. *J Clin Invest*. 2017;127:780–9.
- Chong PK, Lee H, Loh MC, Choong LY, Lin Q, So J, et al. Upregulation of plasma C9 protein in gastric cancer patients. *Proteomics*. 2010;10:3210–21.
- Chantaraamporn J, Champattanachai V, Khongmanee A, Verathamjamras C, Prasongsook N, Mingkwan K, et al. Glycoproteomic analysis reveals aberrant expression of complement C9 and fibronectin in the plasma of patients with colorectal cancer. *Proteomics*. 2020;8:26.
- Zhang Y, Ye QJ, He JX, Chen P, Li X. Recurrence-associated multi-RNA signature to predict disease free survival for ovarian cancer patients. *BioMed Res Int*. 2020;2020:1618527.
- Deng W, Liu HL, Luo S, Clarke J, Glass C, Su L, et al. APOB genotypes and CDH13 haplotypes in the cholesterol related pathway genes predict non-small cell lung cancer survival. *Can Epid Bio Prev*. 2020;29:1204–13.
- Yi GH, Luo HX, Zheng YL, Liu WJ, Wang DN, Zhang Y. Exosomal proteomics: unveiling novel insights into lung cancer. *Aging Dis*. 2024;16:1–25.
- Al-Nedawi K, Meehan B, Kerbel RS, Allison AC, Rak J. Endothelial expression of autocrine VEGF upon the uptake of tumor-derived microvesicles containing oncogenic EGFR. *Proc Natl Acad Sci*. 2009;106:3794–9.
- Taverna S, Giallombardo M, Gil-Bazo I, Paola C, Castiglia M, Chacartegui J, et al. Exosomes isolation and characterization in serum is feasible in non-small cell lung cancer patients: critical analysis of evidence and potential role in clinical practice. *Oncotarget*. 2016;7:28748–60.

Publisher's Note

Springer Nature remains neutral with regard to jurisdictional claims in published maps and institutional affiliations.